



Probabilistic forecasting informed failure prognostics framework for improved RUL prediction under uncertainty: A transformer case study

J.I. Aizpurua^{a,b,*}, B.G. Stewart^c, S.D.J. McArthur^c, M. Penalba^{d,b}, M. Barrenetxea^e, E. Muxika^a, J.V. Ringwood^f

^a Mondragon University, Electronics & Computer Science Department - Signal Theory & Communications, Arrasate, Spain

^b Ikerbasque, Basque Foundation for Science, Bilbao, Spain

^c University of Strathclyde, Department of Electronic and Electrical Engineering - Institute for Energy & Environment, Glasgow, UK

^d Mondragon University, Mechanical & Industrial Production Department - Fluid Mechanics, Arrasate, Spain

^e Mondragon University, Electronics & Computer Science Department - Power Electronics, Arrasate, Spain

^f Maynooth University, Electronic Engineering Department, Maynooth, Ireland

ARTICLE INFO

Keywords:

Condition monitoring
Probabilistic forecasting
Transformer
Prognostics
Uncertainty

ABSTRACT

The energy transition towards resilient and sustainable power plants requires moving from periodic health assessment to condition-based lifetime planning, which in turn, creates new challenges and opportunities for health estimation and prediction. Probabilistic forecasting models are being widely employed to predict the likely evolution of power grid parameters, such as weather prediction models and probabilistic load forecasting models, that precisely impact on the health state of power and energy components. These models synthesize forecasting knowledge and associated uncertainty information, and their integration within asset management practice would improve lifetime estimation under uncertainty through uncertainty-aware probabilistic predictions. Accordingly, this paper presents a probabilistic prognostics method for lifetime planning under uncertainty integrating data-driven probabilistic forecasting models with expert-knowledge based Bayesian filtering methods. The proposed concepts are applied and validated with power transformers operated in two different power generation systems and obtained results confirm that the proposed probabilistic transformer lifetime estimate aids in the decision-making process with informative lifetime distributions and associated confidence intervals.

1. Introduction

Prognostics & Health Management (PHM) is a health management paradigm which encompasses different predictive applications for an improved reliability management of engineering components and systems [1]. PHM is at the hearth of condition monitoring technology, where different monitored datasets cooperate, along with engineering knowledge, to develop anomaly detection, diagnostics, prognostics and maintenance planning applications. For recent reviews see e.g. [2,3].

The main focus of this research is on the development of failure prognostics models, centred on the prediction of the likely future degradation of the asset under study, and the estimation of the associated remaining useful life (RUL). The RUL denotes the time distance from the current prediction time, t_p , to the end of the useful life of the asset (denoted EOL) [4]:

$$RUL = EOL - t_p | EOL > t_p \quad (1)$$

The remaining time after t_p until EOL is random, and therefore, uncertainty modelling is crucial for accurate RUL predictions [5]. Fig. 1 shows the RUL prediction concept, where $Y = \{y_1, \dots, y_n\}$ denotes the gathered data samples up to the prediction point t_p .

In order to design accurate prognostics applications, it is necessary to capture complex and stochastic interactions including the asset degradation and operation conditions. To this end, the prognostics model development covers multiple stages, including data collection, model development and validation, which are surrounded by different sources of uncertainty, such as measurement, model development and parameter estimation uncertainty. The different sources of uncertainty are generally grouped into epistemic and aleatory uncertainty [6]. Epistemic uncertainties cover the lack of complete knowledge, while aleatory or inherent uncertainty models uncertainties which cannot be measured. Generally, it is assumed that epistemic uncertainty is reducible and aleatory uncertainty is irreducible, e.g. see [7].

* Corresponding author at: Mondragon University, Electronics & Computer Science Department - Signal Theory & Communications, Arrasate, Spain.
E-mail address: jiaizpurua@mondragon.edu (J.I. Aizpurua).

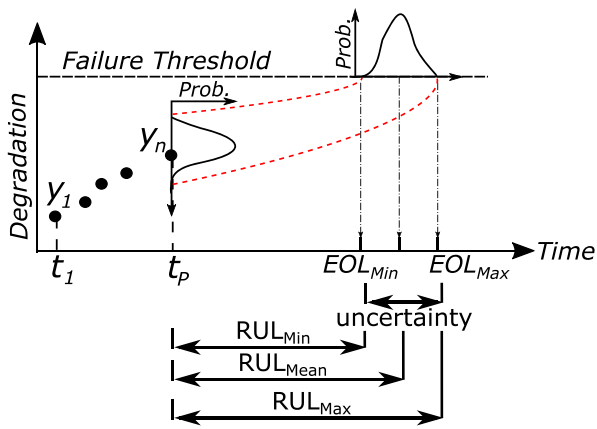


Fig. 1. Remaining useful life prediction [4].

RUL prediction uncertainty is specific to the component or system under study. However, there are key transversal activities which are common to prognostic modelling processes, such as data-measurement, initial state-estimation, degradation process modelling, future operational usage, and failure threshold definition. In Fig. 1, it can be observed that the initial health-state estimate at t_p is uncertain, which is represented by a probability density function (PDF). The progression of this PDF and the distance to EOL depends on the degradation process, the model that is used to describe this trajectory, and the failure threshold. Accordingly, different methodologies have been proposed for the uncertainty quantification associated with RUL estimation.

Specifically, data-measurement uncertainties, along with state-estimation uncertainties, have been widely addressed through different filtering strategies such as extended and unscented Kalman filtering and Bayesian particle filtering [8]. Filtering models iterate through measurement and degradation functions based on observations, physics-based models and sampling strategies. If the degradation process is specified with an analytical model, degradation model uncertainty can be quantified by obtaining the same PDF for every repetition of the algorithm, e.g. using first-order reliability methods [9], Wiener processes [10] or Gamma processes [11]. Different strategies to include uncertainty in the failure threshold criteria have been also analysed [12,13]. For a comprehensive set of examples on uncertainty associated with RUL quantification, the reader is referred to [14].

The different sources of uncertainty, along with complex and sometimes unforeseen scenarios, can lead to discrepancies between observations and predictions, and thereby impact on the RUL estimates and the associated health management decision-making process. In this context, there are different challenges that emerge from the development of accurate prognostics applications [15].

In particular, in the area of power and energy systems, owing to the increasing advent of dynamic and stochastic energy applications, monitoring and reliability applications are rapidly departing from deterministic operation contexts [16,17]. This application context, including renewable energy systems [18] and electric vehicles [19], along with the inherent PHM modelling uncertainties, invalidates the use of deterministic lifetime models owing to the generated dynamics and sources of uncertainty that affect the operation conditions and lifetime management practices [20,21].

Accordingly, it is of utmost importance to properly integrate and propagate uncertainties. If the different sources of uncertainty are not considered from the lowest level up to the system level [22], their effect is lost on the system scale. This may lead difficult asset-management decisions due to the lack of knowledge and control of variables implied in the lifetime prediction. For example, renewable energy forecasting solutions use weather prediction models of natural resources, e.g. wind speed, wave height, and solar irradiance. Individual component-level

predictions are then integrated at the system level, e.g. for wind, wave and solar park level energy predictions. The escalation from component to system level predictions involves uncertainties at different levels, and in the case of renewable energy generation, the generated power directly affects the RUL of different power assets, such as transformers, cables and converters, through the generated power that flows through them.

1.1. State-of-the-art

Recent developments in the prognostics area include the use of novel accurate data-driven methods, which can capture complex non-linear relationships, possibly with memory capabilities, for an improved RUL prediction, such as deep-learning based fusion of prognostics models for turbofan engines [23] — see [24] for an exhaustive review of deep-learning applications for PHM. Data-driven models can generate accurate RUL predictions, however, their ability to account for uncertainties is limited [2,3,15]. Accordingly, recent efforts have been focused on the development of hybrid prognostics models, that combine physics-based models with data-driven models to develop an accurate prognostics model that is able to obtain explainable results, and ideally, also deal with multiple sources of uncertainty [25].

In this direction, Arias et al. presented the combination of physics-based and data-driven deep-learning models for prognostics predictions of a turbofan engine, where the uncertain parameters of the physics-based model are calibrated with observations using a Unscented Kalman Filter (UKF), which is then used as input to a deep-learning based prognostics model [26]. The comprehensive approach deals with uncertainties through the UKF approach using Gaussian distributions. However, the deep-learning model predictions are point-estimates without probabilistic uncertainty information.

Nascimento et al. embedded the physics-based model within the data-driven learning process through a physics-informed neural network approach for prognostics prediction of batteries. Recurrent neural network (RNN) cells are used to capture model uncertainty, which are embedded within the physics-based degradation model of the battery, and an ensemble strategy is used to perform a weighted average of ageing curves of older batteries [27]. RNN model parameters are modelled with Gaussian distribution and processed with variational inference, which enables partially capturing the model development uncertainties. However, measurement uncertainties are not fully captured and the resulting RUL predictions do not include the complete probability density function. Zhang et al. integrated artificial neural network based and physics-based RUL prediction models through weighted RUL predictions for prognostics of railway cables [28]. As with previous models, physics-based models can integrate model uncertainties, but ANN based formulations do not capture uncertainties.

These approaches provide systematic methods to incorporate physics-based models within the degradation formulation, either as input parameter of data-driven prognostics models [26], inter-leaved with the degradation process [27] or through combination of results [28]. The flexibility of the analysed methods comes with a cost, which is the inability to cover the whole range of uncertainties and provide a complete distribution function of uncertainty estimates. This, generally, requires the development of a model, which explicitly captures uncertainties along with the degradation process and propagates them with the degradation model and RUL prediction.

As for the probabilistic prognostics methods, there is an increasing interest on modelling the degradation of complex systems and estimating their RUL [15]. Chiachio et al. presented a Markov-chain based prognostics framework, where Markov-chain models are connected with Particle filter (PF) based state-estimation methods [29]. The measurement equation is comprised of condition data, which is used to update the predictions. The Markov-chain approach can model multi-state degradation processes of complex systems, however, due to the nature of the Markov-chains, the degradation model is limited

by a predefined set of states, with constant exponential transitions and governed by the Markov property, and this limits the uncertainty modelling capabilities.

Si et al. proposed a data-driven prognostics modelling approach for non-linear degradation processes, based on the Box–Cox transform and Wiener process [30]. It is an elegant prognostics framework that, under the adopted assumptions, operates with high precision. However, input signals are assumed deterministic and therefore relevant sources of uncertainty, such as measurement uncertainties, are not integrated. Chen et al. presented a mixture proposal PF for the integration of dynamic crack evolution of multi-crack scenarios [31]. It is a comprehensive framework that can incorporate multiple cracks, model uncertainty is modelled with Gaussian distribution with fixed mean value and variance, and it also integrates prediction results, but still, they are formulated as deterministic estimates of prediction models.

Each of these models pose advantages, such as improved accuracy of deep-learning models, enhanced explicability of physics-based models, and capability to capture complex non-linear degradation processes. However, they also imply other assumptions, e.g. Kalman filter assumes Gaussian noise, RNN models require large amount of data, Markov-chains rely on predefined states and exponential distribution, and more importantly for the purpose of this research, they do not capture uncertainties from other model predictions with a complete PDF.

If the prognostics model is informed by external models that convey degradation-influencing information, e.g. [31], it is crucial to fully propagate predictive information from previous stages. However, using the reviewed methods, this information is partially propagated, or even lost, because they cannot capture and integrate the full probability density function of the modelled process. In order to properly propagate uncertainty, it is generally necessary to model and propagate predictions as full probability distribution functions of plausible values of the estimated parameter consistent with the underlying modelled process.

1.2. Research opportunity

One possibility to model and capture uncertainties is to use probabilistic forecasting models [32]. These models estimate the probability density function (PDF) associated with each prediction instead of a deterministic point estimate. Probabilistic forecasting models are gaining momentum for accurate wind energy [22], solar energy [33] and load estimation models [34]. Most of the forecasting models address the probabilistic prediction task including the integration of uncertainty. However, the interactions between different sources of uncertainty are difficult to capture systematically [15], and the use of these models in PHM applications, requires propagating uncertainties without losing information.

The aggregation and post-processing of the uncertainty information synthesized as PDFs for an enhanced decision-making has been addressed for degradation modelling [35], diagnostics [36], damage modelling frameworks to propagate and evaluate the influence of storms [37], post-contingency power-flow analysis [38] and other application areas [39]. However, in the area of probabilistic forecasting, generally, the probabilistic prediction stage finishes with the predicted probabilistic information and this is not further post-processed for an enhanced decision-making in subsequent modelling stages.

Aligned with methodologies that propagate uncertainty information obtained from probabilistic forecasting methods in the form of PDFs, the main hypothesis of this work is that it is more beneficial to build distributions directly from data, and then post-process this information to perform better informed predictions based on this empirical distribution. To this end, it is necessary to replace measurements with forecasting PDF estimates that integrate different sources of uncertainty through the underlying forecasting technique. This would result in the integration of probabilistic forecasting models within a lifetime estimation framework and it may lead to an improved health state estimation under uncertainty.

1.3. Contribution

Accordingly, this paper introduces a lifetime prediction approach that integrates probabilistic forecasting strategies with experimental lifetime methods, and this is the main contribution with respect to the state-of-the-art. The integration and propagation of uncertainties enables the adaptation of uncertainty-aware lifetime predictions, expressed with the complete PDF of the RUL predictions which represent plausible values of the RUL estimate, consistent with the underlying probabilistic framework. This has a direct impact and applicability for the integration of probabilistic forecasting methods into the proposed approach. The proposed framework is implemented for a transformer lifetime prediction case study and is validated with two different case studies.

The proposed approach extends previous work [40] through the integration of probabilistic forecasting estimates. This is achieved through the replacement of parametrized distributions with data-driven probabilistic forecasting models and their integration with expert-based experimental models in a Bayesian state-estimation framework. It also extends preliminary work in [41] through formalizing the approach and testing with two relevant industrial case studies.

1.4. Organization

The remainder of this paper is organized as follows. Section 2 presents the proposed probabilistic framework for lifetime prediction under uncertainty. Section 3 implements the framework for the specific case of power transformer lifetime estimation, enhancing the traditional thermal and lifetime modelling equations defined by the IEEE standard C57.91. Section 4 applies the methodology to two different power transformer case studies. Finally, Section 5 draws conclusions.

2. Proposed framework for probabilistic forecasting informed failure prognostics

Lifetime evaluation methods estimate the remaining lifetime through experimental equations or data-driven models. These models, generally, make use of monitored datasets and parameters that model the usage and stress profiles along with asset-specific parameters of the lifetime model.

Given the fast and prominent advance of probabilistic forecasting techniques, and their ability to estimate parameters under uncertainty, it is likely that lifetime parameters may be calculated using probabilistic models, so as to anticipate to potential degradation scenarios and assist in decision-making under uncertainty.

Compared with point prediction estimates, with complete probabilistic distribution functions associated with each prediction, error modelling variables are no longer constant and they vary for each prediction.

Accordingly, a probabilistic lifetime estimation approach has been developed which predicts the lifetime using inspection data and probabilistic forecasting estimates. Fig. 2 shows the developed probabilistic lifetime estimation approach.

The probabilistic forecasting approach models the probabilistic evolution of lifetime-influencing variables, *i.e.* stressors, where each individual forecasting model integrates different sources of uncertainty present in the modelled process.

Each individual probabilistic forecasting results are modelled with a complete probability density function, $pdf(t)$, and this PDF includes uncertainty information associated with the prediction of the lifetime-influencing parameter.

The probabilistic forecasting model inputs the probabilistic lifetime model along with other sources of uncertainty, including the initial health state, and the process degradation uncertainty. The outcome of the probabilistic lifetime model is a set of PDFs of the RUL estimate, inferred at different prediction time instants, RUL_i .

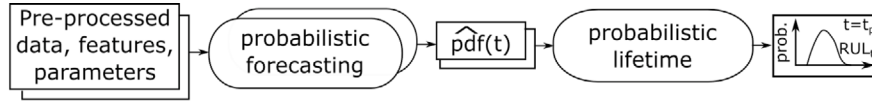


Fig. 2. Probabilistic remaining useful lifetime estimation framework.

The proposed probabilistic lifetime estimation approach is based on the integration of probabilistic forecasting techniques and lifetime modelling formulations through adapted Bayesian state-estimation methods. The rest of this section presents probabilistic forecasting and probabilistic lifetime estimation basics that have been implemented to develop the proposed approach.

2.1. Probabilistic forecasting models

A range of different methods can be employed for the probabilistic forecasting modelling stage [32]. Among existing probabilistic forecasting models, that are able to integrate uncertainties and produce a PDF for each prediction estimate, the application of the proposed probabilistic lifetime methodology focuses on the implementation of Quantile Regression Forest and Quantile Gradient Boosting models with the aim to select the model with the best predictive power [42].

These methods have been selected due to their capability to capture non-linear relationships, including interactions between input features, integration of quantile loss functions, and previous successful experience in other studies [43,44]. However, note that this selection does not limit the proposed framework, and if desired, it is possible to substitute these applications with other probabilistic forecasting algorithms.

These models can be used to create prediction intervals that contain information about the uncertainty of observations around the predicted value. This generates robustness against measurement uncertainties when using probabilistic forecasting results.

2.1.1. Quantile regression forests (QRF)

QRF are based on Random Forests (RF) and they have shown excellent results in different forecasting competitions [43,45]. RF grow a large ensemble of trees using n independent observations $(y, x_i) \in \{1, \dots, n\}$.

QRF are an ensemble of different regression trees in which each leaf draws a distribution for the target variable y . QRFs obtain prediction intervals from RF predictions, which represent the uncertainty of the predicted value, i.e. the greater the uncertainty the greater the prediction interval and vice-versa.

The prediction becomes a conditional distribution function $P(y|X = x_i)$ for $i \in \{1, \dots, N\}$ for $X = x_i, y < y_i \in \mathbb{R}$. The corresponding conditional distribution function $F(y|X = x_i)$ can be also expressed as $E(1_{y < y_i} | x = x_i)$, which is approximated by the weighted mean of x_i over the observations:

$$\hat{F}(y|X = x_i) = \sum_{i=1}^N w_i(x_i) 1_{\{y < y_i\}} \quad (2)$$

where $w_i(x_i) = K^{-1} \sum_{k=1}^K w_i(x_i, \theta_k)$ is the weighted vector and $1_{\{\cdot\}}$ is an indicator function.

The α -quantile, $Q_\alpha(x_i) = \alpha$, is defined such that the probability of $y < Q_\alpha(x_i) = \alpha$. The quantiles give more complete information about the distribution of y as a function of the predictor features X . For instance, for a new feature vector, X_w , 95% prediction intervals for the value of y are given by:

$$I(X_w) = [Q_{0.025}(y|x = X_w), Q_{0.975}(y|x = X_w)] \quad (3)$$

Using quantiles and interpolation methods it is possible to build a CDF and then extract the corresponding PDF.

2.1.2. Quantile Gradient Boosting (QGB)

QGB are based on boosting methods that sequentially combine an ensemble of weak learners as a weighted sum of base-learner models in order to reduce the error of the whole ensemble [46]:

$$\hat{y}_t = F_N(x_t) + \varepsilon_t = \sum_{n=1}^N f_n(x_t) + \varepsilon_t \quad (4)$$

where $F_N(x_t)$ is the ensemble of N regression trees, each $f_n(x_t)$ is a regression tree and ε_t is an error term. The new regression tree $f_{n+1}(x_t)$ for the quantile loss function $L(\cdot)$ is estimated as follows:

$$\underset{f_{n+1}}{\operatorname{argmin}} \sum_t L(y_t, F_N(x_t) + f_{n+1}(x_t)) \quad (5)$$

This optimization is solved through the steepest descent algorithm [46], where the base-learners $f_n(x_t)$ are constructed to be maximally correlated with the negative gradient of the loss function associated with the whole ensemble $F_N(x_t)$.

The implementation of the quantile loss function enables the probabilistic prediction through α -quantiles also known as Quantile Gradient Boosting (QGB) [44].

2.2. Probabilistic lifetime modelling

In order to estimate the asset lifetime under uncertainty, probabilistic forecasting modelling results are integrated with the asset-specific experimental degradation equation.

This integration can be achieved through a modified Particle Filtering (PF) strategy [47]. PF is a state-estimation method that combines Monte Carlo simulations with Bayesian inference.

PF diagnoses the system health state x_t through a iterative combination of the health degradation model $f(\cdot)$ and its influencing measurements $h(\cdot)$:

$$\begin{aligned} x_k &= f(x_{k-1}, w_{k-1}) \\ z_k &= h(x_k, \varphi_k) \end{aligned} \quad (6)$$

where x_k denotes the asset RUL at the discrete time instant k , $f(\cdot)$ is the asset-specific experimental degradation function, w_k is the degradation uncertainty vector, z_k is the lifetime-influencing parameter at time instant k , $h(\cdot)$ is the lifetime-influencing parameter estimation function (also named measurement function), that correlates asset health measurements with the RUL estimate, and φ_k is the measurement uncertainty vector (see application in Section 3.2.3).

So as to integrate probabilistic forecasting estimates with the system health state estimation procedure, the prediction intervals of the forecasting estimates should be aligned with the discrete time-step k of the state-degradation function. For example, if hourly sampled predictions are performed for H discrete steps, this leads to a prediction horizon of $k \times H$ hours.

The PDF $p(x_k | z_{0:k})$ defines the asset health state x_k given measurements z_k up to k . The *prior* PDF of the asset health state x_k from the distribution $p(x_{k-1} | z_{0:k-1})$ is determined by:

$$p(x_k | z_{0:k-1}) = \int p(x_k | x_{k-1}) p(x_{k-1} | z_{0:k-1}) dx_{k-1} \quad (7)$$

where the distribution $p(x_k | x_{k-1})$ is determined from (6). The *posterior* PDF reflects the updated *prior* PDF with new measurements gathered at k , z_k , by using the Bayesian inference:

$$p(x_k | z_{0:k}) = \frac{p(x_k | z_{0:k-1}) p(z_k | x_k)}{p(z_k | z_{0:k-1})} \quad (8)$$

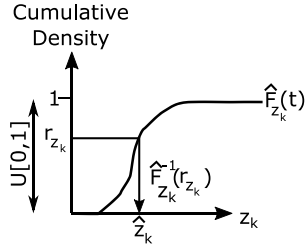


Fig. 3. Inverse transform sampling for probabilistic forecasting results.

The PF method was proposed to solve (8) through iterative application of prediction, update and resampling steps at each time instant k [47], which has been adapted here to include probabilistic forecasting estimates of the measurement function.

At time instant $k = 0$, in order to model the initial transformer health state, N_p random samples, also known as particles, are drawn $\{x_{k=0}^i\}_{i=1}^{N_p}$ from the initial asset health state conditions.

Prediction: the prediction at time instant $k > 0$ is performed by sampling from the distribution of the asset degradation uncertainty w_{k-1} and simulating the asset health degradation dynamics according to (6) to generate new asset health state samples x_k^i which are realizations of the predicted distribution $p(x_k | z_{0:k-1})$.

In order to draw particles from the probabilistic forecasting predicted PDF, $p\hat{d}f_{z_k}(t)$, the inverse sampling method is applied. Let $\hat{F}_{z_k}(t)$ be the cumulative distribution function of the parameter z at discrete time instant k , inferred from the probabilistic forecasting model, r_{z_k} the random variable drawn from the uniform distribution $r_{z_k} \sim U([0, 1])$, then the inverse sampling method applies the relation $\hat{F}_{z_k}^{-1}(r_{z_k}) = \hat{z}_k$. Fig. 3 shows the inverse transform sampling process.

Update: each sampled particle is assigned a weight based on the likelihoods of observations z_k collected at time k :

$$w_k^i = \frac{p(z_k | x_k^i)}{\sum_{j=1}^{N_p} p(z_k | x_k^j)} \quad (9)$$

An approximation of the *posterior* PDF, $p(x_k | z_{0:k})$, is then obtained from the weighted samples $\{x_k^i, w_k^i\}_{i=1}^{N_p}$.

Resampling: so as to avoid the weight degeneracy phenomena [47], where all but one particle have negligible weights, an effective number of particle size is defined: $N_e = 1 / \sum_{i=1}^{N_p} w_k^i$. If N_e falls below a threshold ($N_p/2$ in this work), a systematic resampling step is applied [47].

3. Case study: Transformer probabilistic lifetime estimation under uncertainty

Transformers are key integrative components of the power grid. Health monitoring and reliability assessment of transformers is crucial for the secure and reliable operation of power and energy systems [48]. Transformers are constituted of different systems including tap-changers, bushings and the insulation system.

The solid insulation is a crucial system that can cause the transformer failure [48,49] and it is the focus of this case study. If transformers are operated under predictable and periodic thermal and power conditions deterministic solid insulation lifetime models defined in IEEE standards [49] can be used for health monitoring and reliability assessment.

Transformer lifetime estimation approaches have been focused on the integration of collected measurement into a lifetime estimation model [40,50–53]. Bicen et al. implemented a transformer lifetime monitoring model based on annual load factors [50] and Ariannik et al. developed a lifetime estimation model for transformers based on the degree of polymerization and water levels [51]. These models can convey predictive information based on deterministic experimental

equations. However, the proposed methods lack modelling mechanisms to propagate uncertainty information and their ability to inform decision-making strategies in the presence of uncertainties is limited.

Recent contributions focus on the integration of uncertainty information in the transformer lifetime estimation model [52,53]. Catterson first proposed the integration of uncertainty in the transformer lifetime estimation process [52] and Li et al. developed a diagnostics approach integrating uncertainty information [53]. These models are valid solutions if the measurement data is directly used in the lifetime estimation framework. However, if collected measurements need to be projected into the future, e.g. for prognostics tasks, these models need to integrate and propagate uncertainties [54,55].

In this direction, the main motivation of this case study is the development of a probabilistic lifetime estimation approach through uncertainty management and probabilistic forecasting methods for improved transformer lifetime estimation under uncertainty.

3.1. Transformer degradation modelling

One of the key life-limiting failure modes for power transformers is the ageing of the solid insulation paper [48,49]. The degree of polymerization (DP) of the insulation paper represents the tensile strength of the paper, which is defined as the number of monomeric units, and it is weakened over time. The insulation end-of-life is reached when the DP drops below a threshold level and the insulation integrity is lost. In this situation the transformer cannot withstand operational stresses. New insulation paper has a DP in the interval of 1000–1200 and insulation end-of-life is considered when DP is 200 [56].

The insulation end-of-life is governed by the winding temperature, which in turn, is determined by the load current that flows through the transformer along with ambient temperature and transformer-specific parameters. The influence of humidity in the DP is a studied phenomena [51]. However, this work focuses on the experimental model given in the standard IEEE C57.91 [49] due to the unavailability of water level measurements. There are other indicators, such as the dissolved gasses in oil, that can be used to analyse the insulation health state, but their use for trending the degradation trajectory of the insulation is limited and they are better suited for diagnostics purposes [57].

3.1.1. Lifetime model

The IEEE C57.91 standard defines the insulation paper ageing acceleration factor at time t , $F_{AA}(t)$, as [49]:

$$F_{AA}(t) = e^{\frac{15000}{383} - \frac{15000}{273 + \Theta_H(t)}} \quad (10)$$

where $\Theta_H(t)$ is the transformer winding’s hottest-spot temperature (HST) at time t in °C.

Eq. (10) determines the influence of the HST in the transformer ageing, and the effect on transformer lifetime can be estimated by considering the cumulative effect of HST measurements in the solid insulation over time.

Namely, in order to quantify the transformer remaining useful life at instant t , $RUL(t)$, it is possible to iteratively subtract the fraction of life consumed in each time instant, $F_{AA}(t)$, from the initial health state RUL_0 . Accordingly, Eq. (10) can be converted into a Markovian recurrence relation form:

$$RUL(t) = \begin{cases} RUL_0 & t = 0 \\ RUL(t - \Delta t) - F_{AA}(t) & t > 0 \end{cases} \quad (11)$$

where Δt is the discrete time-step in hours and $F_{AA}(t)$ is defined in (10).

At the instant $t = 0$, RUL_0 denotes the initial health state estimation. In subsequent iterations, the initial estimate is updated with the most up-to-date RUL estimation. If the insulation paper is new, the initial health state may be assumed to be of 180000 h in the conditions stated IEEE C57.91 [49]. Otherwise, experimental analysis of the insulation paper would be needed to determine the degree of polymerization.

3.1.2. Thermal model

The transformer lifetime is directly influenced by the HST as defined in (10). The measurement of HST is complex and it is generally calculated using analytic relations [49]:

$$\Theta_H(t) = \Theta_{TO}(t) + \Delta\Theta_{H,TO}(t) = \Theta_A(t) + \Delta\Theta_{TO,A}(t) + \Delta\Theta_{H,TO}(t) \quad (12)$$

where $\Theta_A(t)$ and $\Theta_{TO}(t)$ are the ambient and Top-Oil (TO) temperatures, respectively, at time instant t , and $\Delta\Theta_{TO,A}(t)$ and $\Delta\Theta_{H,TO}(t)$ are the top-oil and hottest-spot temperature rise over ambient and top-oil temperatures, respectively, at time t .

The steady-state top-oil temperature rise over ambient temperature, at time t , is calculated through:

$$\Delta\Theta_{TO,A}(t) = \Delta\Theta_{TO,R} \cdot [(i(t)/i_r)^2 \gamma + 1] / (\gamma + 1)^n \quad (13)$$

where γ is the ratio of load loss, at rated load, to loss at zero load, $i(t)$ is the transformer load at time t , i_r is the rated load current, and n is a transformer cooling-specific parameter [49].

Similarly, the steady-state hottest-spot temperature rise, over top-oil temperature at time t , is calculated via [49]:

$$\Delta\Theta_{H,TO}(t) = \Delta\Theta_{H,R} \cdot (i(t)/i_r)^{2m} \quad (14)$$

where m is a transformer parameter determined through a lookup table according to the transformer cooling system [49].

3.1.3. Sources of uncertainty

The use of measurement data for HST estimation, such as top-oil temperature and load, may incur sensor data acquisition errors that affect the HST calculation. The incorporation of measurement uncertainties into (12) gives:

$$\Theta_H(t) = (\Theta_{TO}(t) + \varphi_{TO}) + \Delta\Theta_{H,R} \cdot [(i(t) + \varphi_i)/i_r]^{2m} \quad (15)$$

where φ_{TO} denotes the top-oil measurement error and φ_i designates the load measurement error.

Similarly, the paper degradation process in (11) is a stochastic process, and the integration of the influencing sources of uncertainty [52] gives:

$$RUL(t) = \begin{cases} RUL_0 + w_{RUL_0} & t = 0 \\ RUL(t - \Delta t) + w_{RUL_t} - e^{(15000H\mu_t)(\frac{1}{383} - \frac{1}{273 + \Theta_H(t)})} & t > 0 \end{cases} \quad (16)$$

where w_{RUL_t} and w_t are the lifetime and degradation process uncertainties at t respectively, and $\Theta_H(t)$ is defined in (15). Eq. (16) can be seen as a non-linear autoregressive exogenous model with an error term, w_{RUL_t} , and an externally determined variable, $\Theta_H(t)$, that accumulates measurement errors over subsequent RUL iterations. Note that (15) models load and top-oil temperature errors as constants.

Deterministic thermal and lifetime modelling equations [cf. (10), (11)] are widely employed to estimate the lifetime of transformers, e.g. [20,50,51]. However, these formulations do not integrate different sources of uncertainty. The inclusion of the different sources of uncertainty is becoming increasingly important for the accurate lifetime estimation of transformers operated in emerging power and energy system applications, because deterministic RUL and reliability estimates may lead to sub-optimal health monitoring decisions [58,59].

3.2. Probabilistic forecasting informed framework

Transformer lifetime directly depends on the top-oil temperature and input load. If the top-oil temperature and load samples are gathered from monitoring equipment, the data collection uncertainties can be modelled as in (15) through their respective constant error variables φ_{TO} and φ_i .

However, given the advance of probabilistic forecasting techniques, and their ability to estimate parameters under uncertainty, it is likely that top-oil temperature and load may be calculated using probabilistic

Table 1

Definition of statistical features.

Feat.	Definition	Feat.	Definition
M	$x_m = \frac{\sum_{i=1}^N x_i}{N}$	IF	$x_{if} = \frac{\max x_i }{\frac{1}{N} \sum_{i=1}^N x_i }$
K	$x_{kurt} = \frac{\sum_{i=1}^N (x_i - \mu)^4}{(N-1)\sigma^4}$	RMS	$x_{rms} = \sqrt{\frac{\sum_{i=1}^N x_i^2}{N}}$
SK	$x_{sk} = \frac{\sum_{i=1}^N (x_i - \mu)^3}{(N-1)\sigma^3}$	CF	$x_{cf} = \frac{\max x_i }{\sqrt{\frac{1}{N} \sum_{i=1}^N x_i^2}}$

models, so as to anticipate to potential degradation scenarios and assist in decision-making under uncertainty. With probabilistic distributions, error modelling variables are no longer constant and they vary for each prediction.

In this context, the model in (15) requires modifications to incorporate probabilistic predictions. Accordingly, a probabilistic transformer lifetime estimation approach has been developed based on the implementation of the methodology shown in Fig. 2. The proposed framework predicts the transformer lifetime using inspection data and probabilistic forecasting estimates. Fig. 4 shows the developed probabilistic transformer lifetime estimation approach.

The probabilistic thermal model extends (15) to integrate and propagate probabilistic prediction results in the HST estimation. The model predicts the PDF of the HST, $pd f(t)_{\Theta_H}$, and inputs the probabilistic lifetime modelling phase along with other sources of uncertainty, including the initial health state, $pd f(t)_{RUL_0}$, and the process degradation uncertainty, $pd f(t)_{\omega}$.

Accordingly, in order to estimate the transformer RUL using probabilistic forecasting results, the RUL formulation in (16) needs to be adapted with the proposed approach in Fig. 4. The outcome of the probabilistic framework will be the PDF of the transformer RUL, $\hat{pd} f(t)_{RUL}$.

The proposed probabilistic RUL estimation approach is based on experimental thermal and lifetime modelling formulations along with probabilistic forecasting techniques and adapted Bayesian state-estimation methods. The next sections cover the main phases of the proposed approach (cf. Fig. 4).

3.2.1. Data preprocessing & feature selection

Driven by previous experience [40], different statistical features have been extracted to improve the prediction capability of the probabilistic forecasting models including mean (M), kurtosis (K), impulse factor (IF), root mean square (RMS), skewness (SK), and crest factor (CF). Apart from well-known RMS and mean values, the crest factor evaluates changes in the peak values, impulse factor evaluates the height of a peak, skewness evaluates the asymmetry of a signal distribution and kurtosis evaluates length of the tails of a signal distribution. Table 1 defines the statistical features for N data samples.

A recursive feature elimination (RFE) procedure has been then applied to select the features that minimize the prediction error. RFE is a feature selection method that removes correlated variables that increase the prediction error using a recursive iteration process [60,61].

The main criteria to evaluate the probabilistic forecasts of each model has been the continuously ranked probability score (CRPS). Based on the probabilistic forecast PDF, $f(z)$, with its cumulative distribution function (CDF), $F(z)$, and observation y , the $CRPS(F, y)$ is defined as [62]:

$$CRPS(F, y) = \int_{\mathbb{R}} (F(z) - \mathbb{1}\{y \leq z\})^2 dz \quad (17)$$

where $\mathbb{1}\{y \leq z\}$ denotes the indicator function which is one if $y \leq z$ and zero otherwise.

Namely, the CRPS calculates the discrepancy between the forecast CDF F and the empirical CDF of the observation $\mathbb{1}\{y \leq z\}$ which is considered as a step function because the observations y are deterministic point values.

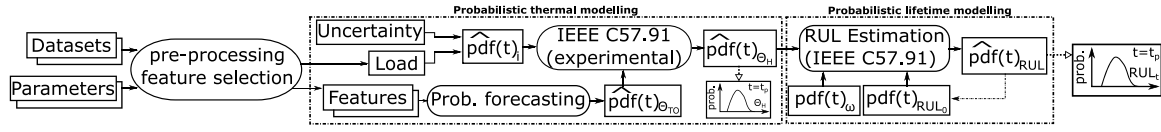


Fig. 4. Probabilistic remaining useful lifetime estimation framework.

The CRPS is a better suited metric for categorizing the predictive power of probabilistic models that generate a PDF as a prediction output because it quantifies the error of each probabilistic predictive value with respect to the observation [63]. In contrast, other metrics such as the root mean square error (RMSE) are based on deterministic point estimate error values and, thus, they have to quantify the RMSE value for every quartile so as to have an overall idea of the predictive power of the model under study.

3.2.2. Probabilistic thermal modelling

The HST of the transformer oil is the most important transformer insulation degradation factor [cf. (16)]. The probabilistic thermal modelling phase aims to predict the HST under uncertainty. This is performed in two connected steps (i) top-oil temperature prediction via probabilistic forecasting models and (ii) HST estimation via experimental models.

Namely, individual probabilistic top-oil temperature forecasts are modelled with a probability density function, $p\hat{d}f(t)_{\theta_{TO}}$. This PDF includes uncertainty information associated with the prediction of the top-oil temperature. In order to estimate the HST using top-oil temperature predictions, (15) is redefined as follows:

$$p\hat{d}f(t)_{\theta_H} = p\hat{d}f(t)_{\theta_{TO}} + \Delta\Theta_{H,R}[(i(t) + \varphi_i)/i_R]^{2m} \quad (18)$$

where $p\hat{d}f(t)_{\theta_H}$ is the PDF estimate of the hottest-spot temperature at instant t , $p\hat{d}f(t)_{\theta_{TO}}$ denotes the probabilistic TOT forecasting outcome at instant t , and $i(t)$, φ_i , i_R , $\Delta\Theta_{H,R}$ and m are defined immediately above.

3.2.3. Probabilistic lifetime modelling

The goal of this phase is the transformer solid insulation RUL estimation under uncertainty. To this end, probabilistic forecasting model results from the thermal modelling phase are connected with experimental degradation equations. This is achieved through a modified PF strategy, which integrates prediction, update and resampling steps as defined in Section 2.2.

PF diagnoses the transformer health state x_k through a iterative combination of the health degradation model $f(\cdot)$ and its influencing measurements $h(\cdot)$, where x_k is the transformer RUL at the discrete time instant k , $f(\cdot)$ is the solid insulation degradation function [defined in (16)], w_k is the degradation uncertainty vector $w_k = \langle w_1, w_{RUL_k} \rangle$, z_k is the HST at time instant k , $h(\cdot)$ is the HST estimation function that correlates transformer health measurements with the RUL estimate [defined in (18)], and φ_k is the measurement uncertainty vector $\varphi_k = \langle \varphi_i \rangle$.

The HST model in (18) integrates load measurements (i), measurement errors (φ_i), probabilistic distribution of the top-oil temperature forecasting estimate including uncertainties ($p\hat{d}f(t)_{\theta_{TO}}$) along with transformer design parameters, and it estimates the distribution function of the HST, $p\hat{d}f(t)_{\theta_H}$.

The solid insulation degradation function modelled in (16) integrates the process noise w_i and calculates the solid insulation RUL from the HST and initial health state, which is then iteratively updated with the actual health state.

At time instant $k = 0$, in order to model the initial transformer health state, N_p random samples, also known as particles, are drawn $\{x_{k=0}^i\}_{i=1}^{N_p}$ from the initial transformer insulation health state conditions. Without loss of generality, throughout this work $N_p = 5000$ particles have been used. See [64] for a extended discussion on the performance of the PF with respect to accuracy and computational time.

At time instant $k > 0$, the predictions are performed by sampling from the distribution of the transformer degradation uncertainty w_{k-1} and simulating the solid insulation degradation dynamics according to (6) to generate new transformer health state samples x_k^i which are realizations of the predicted distribution $p(x_k | z_{0:k-1})$.

In order to draw particles from the predicted probability distribution function of the HST, $p\hat{d}f_{\theta_H}(t)$, the inverse sampling method is applied as defined in Fig. 3, replacing z_k with Θ_H . This sampling method uses the cumulative distribution function, $\hat{F}_{\Theta_H}(t)$, which is inferred from the prediction of the probabilistic forecasting model $p\hat{d}f_{\theta_H}(t)$, to draw samples from the predicted distribution.

In the developed case studies, hourly sampled top-oil and hottest-spot temperature predictions are performed which are aligned with the discrete time-step k of the state-degradation function.

4. Experimental results

This section analyses two power transformers operated in different nuclear power stations through the same probabilistic analysis methodology including data processing, probabilistic thermal modelling and probabilistic lifetime modelling steps.

4.1. Analysis methodology

The data processing stage consists of data cleaning, organization and feature selection steps. Data cleaning and organization steps preprocess datasets by filtering out invalid readings such as erroneous and missing values. The feature selection step is focused on the recursive feature elimination (RFE) procedure [60,61] and the CRPS is used to rank the results and select the best model and its features [cf. (17)].

The probabilistic models have been designed based on the set of explanatory variables that influence analytic relations introduced in Section 3.1. In order to quantify and generalize the predictive power of different probabilistic forecasting models a 10 fold cross-validation (CV) strategy has been used [65].

To this end, available datasets are divided into 10 folds $\{\text{fold}_0, \dots, \text{fold}_9\}$. First, a probabilistic forecasting model is trained for the first fold $\{\text{fold}_0\}$ and tested with the second fold $\{\text{fold}_1\}$. Next, the same model is trained with two folds $\{\text{fold}_0, \text{fold}_1\}$ and tested with the third fold $\{\text{fold}_2\}$ and the process continues until the models are trained with nine folds $\{\text{fold}_0, \dots, \text{fold}_8\}$ and tested on the tenth fold $\{\text{fold}_9\}$. This CV strategy enables the generalization of the predictive performance results by examining the models under different training and testing scenarios. The number of folds incurs a bias-variance tradeoff compromise and 10-fold CV have been shown to yield error estimates that suffer neither from high bias, nor high variance [66,67]. Vertical dashed lines in the available datasets indicate the equidistant folds (Figs. 5, 10).

The power transformer RUL estimation process is based on the PF algorithm. Based on expert knowledge [49], the initial state of the solid insulation paper is modelled as a new paper with 180 000 h with an 8% uncertainty from the initial lifetime. The process noise is modelled with a variation of 0.01% from the initial lifetime (cf. Table 2). These are plausible assumptions adopted for experimentation purposes, but note that they do not limit the applicability of the approach.

The three scenarios displayed in Table 3 have been studied and compared when estimating the RUL. Configuration #1 is the deterministic model that uses measured top-oil temperature and load data as in the

Table 2
Probabilistic assumptions of noise and initial state.

Model parameter	Symbol	Distribution
Initial state	$RU L_0$	$N(180000, 150)$
Process noise	w_k	$N(0, 20)$

Table 3
Transformer RUL evaluation configurations.

ID	RUL	HST	Top-oil temperature	Load
#1	Eq. (11)	Eq. (12)	$\hat{\theta}_{TO} = \theta_{TO}(t)$	$\hat{i} = i(t)$
#2	Eq. (16)	Eq. (15)	$\hat{\theta}_{TO} = N(\theta_{TO}, \varphi_{TO}), \varphi_{TO} = 5\%$	$\hat{i} = N(i, \varphi_i), \varphi_i = 5\%$
#3	Eq. (16)	Eq. (18)	$\hat{\theta}_{TO} = p\hat{\delta} \int_{\theta_{TO}}(t)$	$\hat{i} = N(i, \varphi_i), \varphi_i = 5\%$

Table 4
Parameters of the analysed EDF power transformer.

Param.	Value	Param.	Value	Param.	Value
Cooling /m,n	Oil Forced Water Forced /0.8,0.9	Rating	735 MVA	$\Delta_{H,R}/\Delta_{TO,R}$	30 °C/ 24.3 °C
V_1/V_2	23 kV/ 400√3 kV	$w_{core,coil} + w_{tank}$	265000 kg	i_r/γ	18.45 kA/0.25

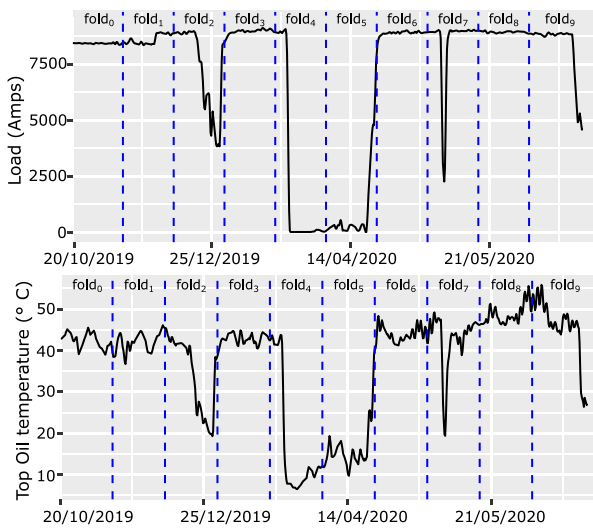


Fig. 5. Monitored load and top-oil temperature (10/2019–06/2020).

standard IEEE C57.91 [49], and its variations [50,51]. Configuration #2 draws measurement errors from the Gaussian distribution for top-oil temperature and load as in [40,52,53]. Configuration #3 is the application of the framework in Fig. 4 with probabilistic top-oil temperature forecasting results and load-measurement errors drawn from the Gaussian distribution.

Results are normalized with the maximum RUL value to generate intuitive metrics and facilitate the decision-making.

4.2. EDF energy power station

The main design and nameplate rating parameters of the power transformer located at a EDF's power station in the UK are displayed in Table 4.

Monitored parameters in the plant include 4-hourly sampled ambient temperature, load, bottom-oil and top-oil temperature. After pre-processing the available datasets, Fig. 5 shows the load and top-oil temperature data of the power transformer.

Fig. 6a shows the mean and standard deviation CRPS values of QRF and QGB models trained with different number of features through 10

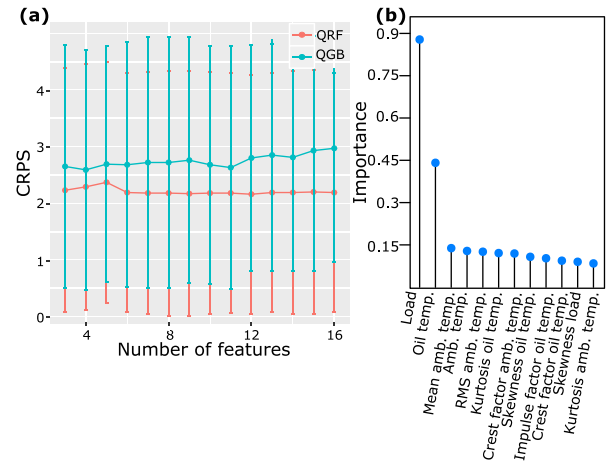


Fig. 6. (a) CRPS results for QRF & QGB models with different features; (b) importance ranking of features for the QRF model.

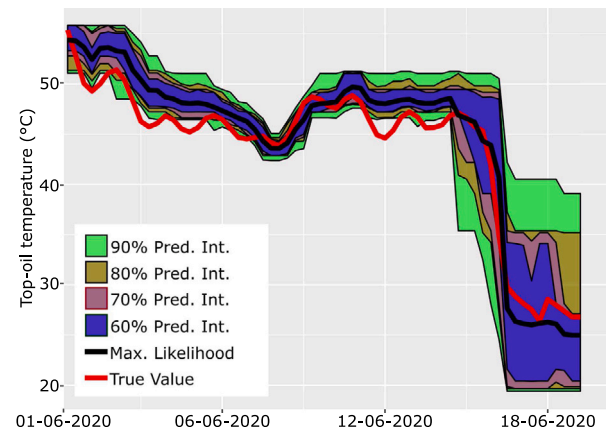


Fig. 7. QRF-based probabilistic top-oil temperature forecasting results.

fold CV, where each fold is comprised of approximately 22 days (cf. Fig. 5). Among the tested models it can be seen that the best performance is obtained with the QRF model with 12 features (CRPS = 1.66 ± 2.1). The best QGB model is obtained with 4 features (CRPS = 1.8 ± 2.17). Fig. 6b shows the importance of the best probabilistic forecasting model features, i.e. QRF model with 12 features. It can be observed that the load and bottom oil temperature have the greatest importance, as defined in the analytic relation in (12), substituting the ambient temperature with the bottom-oil temperature, which is more informative, but less commonly monitored. The remaining features, including ambient temperature, describe the dynamics not captured by these features and the model in (12). Accordingly, subsequent forecasting and lifetime estimation steps will be based on this QRF configuration.

After selecting the features of the QRF model, the model is trained using the first 7 folds and tested on the last 3 folds. The QRF model estimates the conditional quantiles of the top-oil temperature given input features. Fig. 7 shows the top-oil temperature maximum likelihood estimates, different prediction intervals and the true value for the last fold.

Fig. 7 shows that the maximum likelihood value persistently follows the true value. The uncertainty of the QRF model in each prediction determines the width of different prediction intervals. That is, if the QRF model is confident in the prediction, the prediction bounds are narrow (around 06-06-2020). In contrast, if the QRF model is not confident in the predictions, the prediction bounds are wider (around

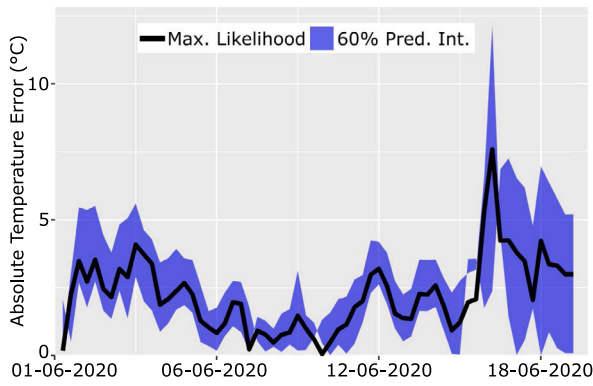


Fig. 8. Absolute top-oil temperature estimation errors from Fig. 7.

18-06-2020). This can be visually checked in Fig. 7, where prediction bounds increase with the prediction horizon.

The uncertainty area for decision-making depends on the predicted PDF and the prediction interval. That is, 90% prediction intervals cover most of the area of the predicted PDF, but if the width of the PDF is wide, then the decision making area will be also wide. In contrast, if the width of the PDF is narrow, it may be the case that low prediction intervals cover most of the area of the PDF. The width of the PDF is reflected on the prediction intervals shown in Fig. 7.

Fig. 8 shows the absolute top-oil temperature estimation error along with the 60% prediction intervals for the probabilistic top-oil temperature forecasts shown in Fig. 7.

It can be seen that the width of the prediction interval varies for different predictions, which informs that the underlying PDF also changes. These uncertainty-aware predictions assist the engineers in the decision-making process with temperature forecasts along with informative prediction intervals.

The three lifetime analysis configurations have been tested for the datasets shown in Fig. 5 (cf. Table 3). Accordingly, Fig. 9 shows the normalized transformer lifetime estimates for the analysed scenarios with the deterministic estimate for the scenario #1, and maximum likelihood RUL estimates along with 95% confidence intervals for the scenarios #2 and #3.

Fig. 9 also shows the PDFs of the health state of the transformer at two different time instants. On the one hand, the diagnostics stage evaluates the health state at the time instant 20-06-2020 by processing all the available data. On the other hand, the prognostics stage predicts the health state in the following 32 months by repeatedly processing the same load and temperature data trajectories from the diagnostics stage four times indicated by vertical dashed lines in Fig. 9.

In each iteration over the available datasets (indicated with vertical lines) it is possible to distinguish two flat periods with almost no degradation that match with the change of operations in the plant (cf. Fig. 5) around December (fold₂) and March–April (fold₄, fold₅). Similarly, the slope of the degradation trajectory towards the summer is greater due to the increased top-oil temperature (fold₈, fold₉).

The degradation trajectory of the configuration based on the Gaussian distribution degrades faster compared with the model based on probabilistic forecasting. The different arises from the underlying PDF used for modelling the top-oil temperature. While Gaussian PDF is based on an assumption of a constant noise added through the Gaussian PDF, the QRF model adapts its prediction bounds according to the confidence in each prediction. In this case the accuracy of the probabilistic model is high (cf. Fig. 6a), and accordingly, the confidence bounds of the probabilistic predictions are narrow (cf. Fig. 7).

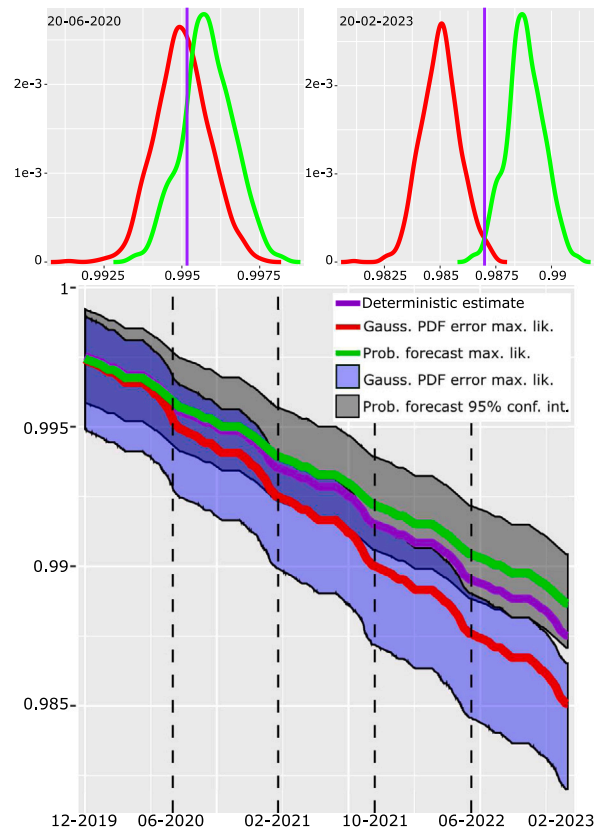


Fig. 9. Transformer RUL estimates for the analysed scenarios.

Table 5

Parameters of the analysed Bruce Power transformer.

Param.	Value	Param.	Value	Param.	Value
Cooling /m,n	Oil Directed Water Forced/1, 1	Rating	267 MVA	$\Delta_{H,R}$	30 °C/
				$\Delta_{T,O,R}$	24.3 °C
V_1 / V_2	17 kV/ $230\sqrt{3}$ kV	$w_{core,coil}$ / w_{tank}	95254 kg/ 30617 kg	i_r/γ	15.1 kA/0.25

4.3. Bruce power station

The main design and nameplate rating parameters of the power transformer located at Bruce Nuclear generating station (Canada) are displayed in Table 5.

Monitored variables include hourly sampled ambient temperature, cooling water temperature, load and top-oil temperature. Fig. 10 shows the preprocessed load and top-oil temperature data for the power transformer.

Fig. 11a shows the mean and standard deviation CRPS values of QRF and QGB models trained and tested with different number of features through 10 fold CV, where each fold is comprised of approximately 138 days (cf. Fig. 10). Among the tested models the best performance is obtained with the QRF model with 13 features (CRPS=4.91 ± 1.5). The best QGB model is obtained with 13 features (CRPS=5.7 ± 1.5). Fig. 11b shows the importance of the best probabilistic forecasting model features, i.e. QRF model with 13 features.

It can be observed that input power and ambient temperature have the greatest importance, which matches with the initial analytic formulation in (12), where top-oil is estimated from ambient temperature and input load. The remaining features, as in the previous case study, describe the dynamics not captured by the model in (12). Accordingly,

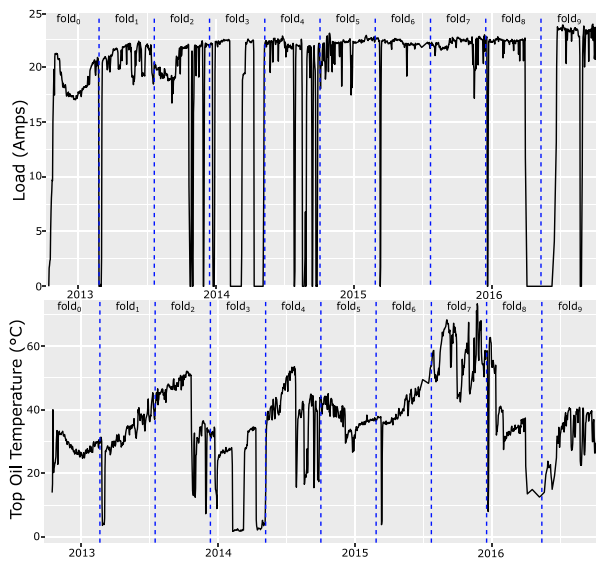


Fig. 10. Monitored load and temperature data (11/2012-10/2016).

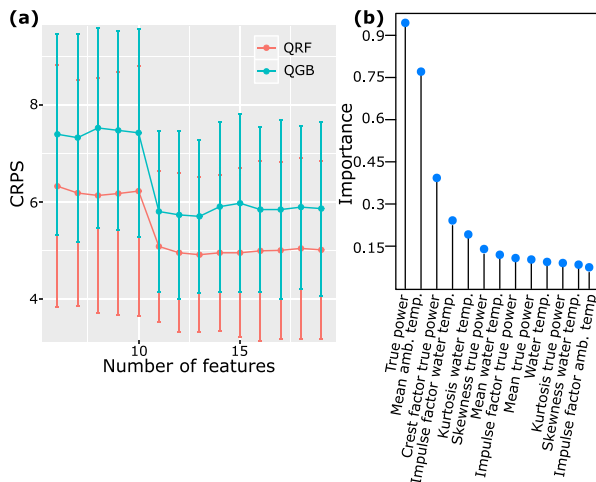


Fig. 11. (a) CRPS results for QRF & QGB models with different features; (b) importance ranking of features for the QRF model.

subsequent forecasting and lifetime estimation steps will be based on this QRF configuration.

After selecting the input features of the QRF model, the model is trained using the first 7 folds and tested on the last 3 folds. The QRF model estimates the conditional quantiles of the top-oil temperature given input features. Fig. 12 shows the probabilistic top-oil temperature maximum likelihood estimates along with different prediction intervals and the true values for the last year of operation, i.e. fold₈ and fold₉.

Fig. 12 shows that the maximum likelihood follows the true value and the associated prediction intervals vary according to the adopted quantiles. That is, the wider the bounds, the wider the area around the maximum likelihood value. Note again that the prediction intervals are not symmetric around the maximum likelihood value, which informs that the estimated PDFs are not Gaussian.

Fig. 13 shows the absolute top-oil temperature estimation errors for 60% prediction intervals along with the maximum likelihood for the probabilistic forecasts in Fig. 12.

It can be seen that the width of the prediction interval increases with the prediction horizon. The power outage causing decreased top-oil temperature between fold₈ and fold₉ causes an increased prediction error because this trend is not captured in the training set. Previous

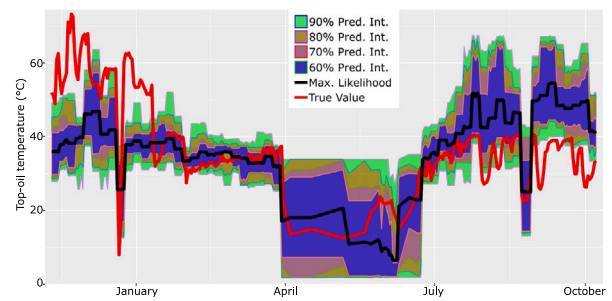


Fig. 12. QRF-based probabilistic top-oil temperature forecasting results.

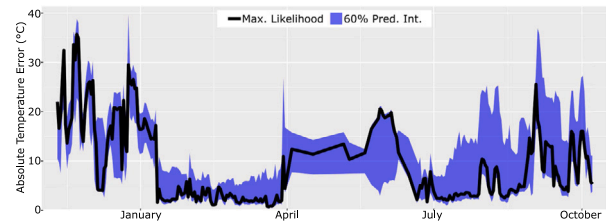


Fig. 13. Absolute top-oil temperature estimation errors from Fig. 12.

power outages in fold₃ cause a more abrupt decrease of the top-oil temperature (cf. Fig. 10).

The three lifetime analysis configurations have been tested for the datasets shown in Fig. 10 (cf. Table 3). All the configurations have been tested with the entire dataset processed sequentially twice including a diagnostics and prognostics stage. Fig. 14 shows the normalized transformer lifetime estimates for the deterministic estimate modelled in configuration #1 and maximum likelihood RUL and 95% confidence intervals for the scenarios #2 and #3. Vertical dashed line indicates the end of the diagnostics stage, i.e. first pass of the available datasets.

Fig. 14 also shows the PDFs of the health state of the transformer at two different time instants. On the one hand, the diagnostics stage evaluates the health state at the time instant 15-10-2016 by processing all the available data. On the other hand, the prognostics stage predicts the health state in the following 4 years by processing the same load and temperature data trajectories from the diagnostics stage.

From the applied load and temperature profiles (cf. Fig. 10) it can be seen that there are three increasing top-oil temperature trends (fold₁ to fold₂; fold₄; and fold₆ to fold₇) interspersed with decreased top-oil temperatures (fold₃; fold₄; and fold₈) that match, respectively, with accelerated degradation trajectories and negligible degradation stages.

Additionally, Fig. 14 shows that probabilistic configurations result in different maximum likelihood and confidence interval values. This is again directly linked with the underlying PDFs used for each configuration (cf. Table 3). Accordingly, although the applied datasets are identical, the underlying distributions of the probabilistic estimates are different, and this has a direct effect on the lifetime estimate. Namely, each of the RUL estimates in Fig. 14 for the configurations #2 and #3 are probabilistic predictions with its corresponding PDF for each of the evaluated discrete time instants and the lifetime estimate of the configuration #1 does not include confidence intervals and therefore there is no criteria for decision-making under uncertainty.

The degradation rate of the configuration #2 is greater compared with the other configurations, and the degradation rate of the configuration #3 is the smallest. This is directly linked with the uncertainty bounds and the maximum likelihood estimate of the underlying PDF. That is, the variance of the measurement data integrated in the Gaussian model (configuration #2) is constant in each iteration and the variance of the PDF of the top oil temperature depends on the uncertainty associated with the prediction of the QRF model (configuration #3).

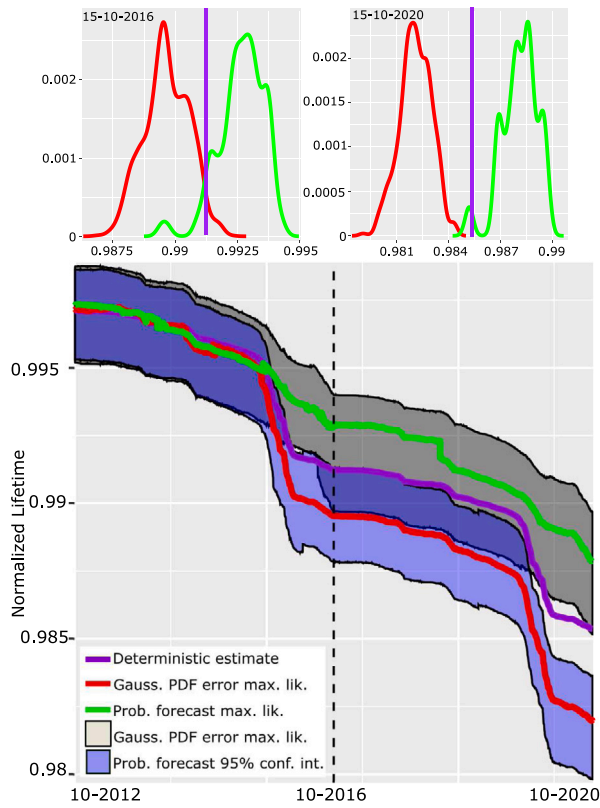


Fig. 14. Transformer RUL estimates for the analysed scenarios.

4.4. Discussion

Among the tested datasets it can be seen that the CRPS values in Figs. 6 and 11 are different. That is, the accuracy of the probabilistic forecasting model of the QRF configuration in Fig. 6 is greater. This translates to probabilistic predictions with smaller uncertainty (cf. Figs. 7 and 12) and lifetime models with smaller uncertainty (cf. Figs. 9 and 14).

Comparing probabilistic models drawn from Gaussian distributions and the designed QRF models in Figs. 9 and 14, it can be observed that the shapes of the PDFs of the RUL predictions are different. The PDF inferred from the QRF model, $p_{\hat{d}}f_{\theta_{T_0}}$, changes for each iteration, while the PDF inferred from the Gaussian distribution is held constant throughout the lifetime estimation. This results in different normalized lifetime estimates including the maximum likelihood and confidence interval values. Note that the different sources of uncertainty of different configurations are further propagated through the same PF framework to estimate the transformer RUL.

Additionally, note that the information provided by the deterministic estimate is a single point value without uncertainty information (cf. Table 3, configuration #1). In these conditions, if the end-user adopts the deterministic model for decision-making about transformer health, maintenance judgements will be solely based on a single-point estimate over the course of the evaluation period. However, the operation of transformers is influenced by different sources of uncertainty and it is important to include them in the lifetime model to quantify their effect on the transformer health and adopt informed decisions accordingly.

Probabilistic thermal and lifetime estimates inform the engineer about the model's forecasting confidence with respect to experienced operational conditions. The greater the forecasting confidence, the narrower the prediction interval of the forecasting estimate as it resembles an experienced operation context, e.g. see 06/06–12/06 period in Fig. 7 and mid-January–April period in Fig. 12, where the features used to

predict these intervals (Figs. 6, Fig. 11) match with the features used to train the forecasting models inferred from training datasets (fold₀-fold₇ in Figs. 5 and 10). This is propagated to the lifetime models along with the constant load error (cf. configuration #3 in Table 3) and results in the PDF estimates shown in Figs. 9 and 14. The width of the lifetime PDF estimates is the result of the integration of the considered sources of uncertainty (initial state, process uncertainty, measurement uncertainty) through the PF-based state estimation algorithm.

The improved prediction accuracy of the state-of-the-art machine-learning models, such as deep-learning, comes at a cost related to the inability to reason about a model's uncertainty and the inability to estimate a complete PDF of the predicted values. While these models may generate accurate prediction estimates, and they may have been used to estimate measurement information, e.g. transformer top-oil temperature (cf. Figs. 7 and 12), their integration in the framework deviates from the proposed approach because they cannot provide a full PDF estimate, and, accordingly, the proposed probabilistic thermal model becomes deterministic. Therefore, deep-learning models may not benefit from the proposed framework due to the missing uncertainty information.

Nevertheless, inspired by the seminal work in [68], probabilistic deep-learning models are emerging [69], and early results combining deep-learning with Bayesian modelling approaches have been proposed, e.g. [70,71]. This suggests that the proposed framework may have a broader impact with the incorporation of additional probabilistic prediction methods.

5. Conclusions

The design of accurate prognostics models requires modelling complex and stochastic interactions including the asset degradation and operation conditions. In the context of power and energy systems, owing to the increasing advent of dynamic and stochastic applications, such as renewable energy systems and electric vehicles, the operation conditions and degradation trajectories are influenced by different sources of uncertainty. This scenario highlights that uncertainty management solutions are needed for accurate asset management practices.

Probabilistic forecasting applications are emerging as potential data-driven solutions for uncertainty-aware predictions. Probabilistic models predict a PDF with a high maximum likelihood and narrow prediction intervals for those instances when the input features are correlated with the training data. In contrast, for unseen features, they predict distributions with low maximum likelihood and wide intervals. The shape of the distribution, i.e. maximum likelihood and prediction intervals, inform the decision-making process indicating the confidence of the probabilistic model on the predictions.

The capability to post-process the probabilistic forecasting model information and integrate in a lifetime estimation framework provides the opportunity to accurately model subsequent decision-making processes. Accordingly, this paper presents a probabilistic forecasting informed failure prognostics framework for the uncertainty-aware RUL estimation based on the integration of probabilistic forecasting models with Bayesian state-estimation methods.

The use of probabilistic models enables the adoption of uncertainty-aware decisions inferring most likely, worst-case and best-case operation scenarios where the prediction intervals vary depending on the effect of uncertainties on the lifetime of the analysed asset. The proposed lifetime prediction framework operates with probabilistic forecasting models designed through a supervised learning process. That is, the forecasting model is designed to optimize the estimation of the expected output prediction with a set of input features. Without probabilistic models, this would lead to deterministic predictions with single point estimates without uncertainty information.

The proposed methodology has been validated through two different power transformer case studies with datasets collected in two

different nuclear power stations. Transformers are key integrative assets of energy systems and their correct operation determines the reliable operation of the power network. However, in order to leverage the potential of the probabilistic forecasting methods for transformer lifetime prediction practices, it is necessary to modify existing transformer lifetime estimation models and integrate the information of probabilistic operation scenarios.

Accordingly, the proposed approach should be useful to evaluate the transformer lifetime in different contexts given different hypothetical operational profiles. In this situation, the framework provides a criteria to evaluate the lifetime reduction of power transformers including different sources of uncertainty.

The operation condition of nuclear power plants includes power outages for maintenance purposes. Power outages lead to different operation states and associated variation of the degradation rates of the transformer. In the context of renewable energy sources, due to the dependence on the intermittent weather conditions and the inherent stochastic nature, the operation states go through more variations. In this context, future work may focus on the adaptation of the framework for renewable energy source applications and the integration of probabilistic load forecasting results.

CRedit authorship contribution statement

J.I. Aizpurua: Conceptualization, Methodology, Software, Data curation, Writing – original draft, Writing – review & editing. **B.G. Stewart:** Resources, Data curation, Writing – review & editing. **S.D.J. McArthur:** Resources, Writing – review & editing. **M. Penalba:** Writing – review & editing. **M. Barrenetxea:** Resources. **E. Muxika:** Visualization. **J.V. Ringwood:** Writing – review & editing.

Data availability

The authors do not have permission to share data.

Acknowledgements

The authors gratefully acknowledge Brandon Lambert from Bruce Power and Martin Kearns from EDF Energy for their supply of transformer data. J. I. Aizpurua is funded by Juan de la Cierva Incorporacion Fellowship (Spanish State Research Agency - grant number IJC2019-039183-I) and partially supported by the Basque Government, Spain (ELKARTEK KK-2021-00021).

References

- Vachtsevanos G, Lewis F, Roemer M, Hess A, Wu B. Intelligent fault diagnosis and prognosis for engineering systems. John Wiley & Sons, Inc.; 2007. <http://dx.doi.org/10.1002/9780470117842>.
- Hu Y, Miao X, Si Y, Pan E, Zio E. Prognostics and health management: A review from the perspectives of design, development and decision. *Reliab Eng Syst Saf* 2022;217:108063. <http://dx.doi.org/10.1016/j.res.2021.108063>.
- Kordestani M, Saif M, Orchard ME, Razavi-Far R, Khorasani K. Failure prognosis and applications—A survey of recent literature. *IEEE Trans Reliab* 2021;70(2):728–48. <http://dx.doi.org/10.1109/TR.2019.2930195>.
- Aizpurua J, Catterson V, Papadopoulos Y, Chiacchio F, D'Urso D. Supporting group maintenance through prognostics-enhanced dynamic dependability prediction. *Reliab Eng Syst Saf* 2017;168:171–88. <http://dx.doi.org/10.1016/j.res.2017.04.005>, Maintenance Modelling.
- Sankararaman S. Significance, interpretation, and quantification of uncertainty in prognostics and remaining useful life prediction. *Mech Syst Signal Process* 2015;52–53:228–47. <http://dx.doi.org/10.1016/j.ymsp.2014.05.029>.
- Bedford T, Cooke R, et al. Probabilistic risk analysis: foundations and methods. Cambridge University Press; 2001.
- Kim S, Choi J-H, Kim NH. Inspection schedule for prognostics with uncertainty management. *Reliab Eng Syst Saf* 2022;222:108391. <http://dx.doi.org/10.1016/j.res.2022.108391>.
- Jouin M, Gouriveau R, Hissel D, Péra M-C, Zerhouni N. Particle filter-based prognostics: Review, discussion and perspectives. *Mech Syst Signal Process* 2016;72:2–31.
- Sankararaman S, Daigle MJ, Goebel K. Uncertainty quantification in remaining useful life prediction using first-order reliability methods. *IEEE Trans Reliab* 2014;63(2):603–19. <http://dx.doi.org/10.1109/TR.2014.2313801>.
- Yu W, Tu W, Kim IY, Mechefske C. A nonlinear-drift-driven Wiener process model for remaining useful life estimation considering three sources of variability. *Reliab Eng Syst Saf* 2021;212:107631. <http://dx.doi.org/10.1016/j.res.2021.107631>.
- Salem MB, Fouladirad M, Deloux E. Variance Gamma process as degradation model for prognosis and imperfect maintenance of centrifugal pumps. *Reliab Eng Syst Saf* 2022;223:108417. <http://dx.doi.org/10.1016/j.res.2022.108417>.
- Acuña-Ureta DE, Orchard ME, Wheeler P. Computation of time probability distributions for the occurrence of uncertain future events. *Mech Syst Signal Process* 2021;150:107332. <http://dx.doi.org/10.1016/j.ymsp.2020.107332>.
- Aizpurua JI, Catterson VM, Abdulhadi IF, Garcia MS. A model-based hybrid approach for circuit breaker prognostics encompassing dynamic reliability and uncertainty. *IEEE Trans Syst Man Cybern: Syst* 2018;48(9):1637–48. <http://dx.doi.org/10.1109/TSMC.2017.2685346>.
- Sankararaman S, Mahadevan S, Orchard ME. Uncertainty in PHM. *Int J Prognost Health Manag* 2020;6(4). <http://dx.doi.org/10.36001/ijphm.2015.v6i4.2289>.
- Zio E. Prognostics and health management (PHM): Where are we and where do we (need to) go in theory and practice. *Reliab Eng Syst Saf* 2022;218:108119. <http://dx.doi.org/10.1016/j.res.2021.108119>.
- Panda DK, Das S. Smart grid architecture model for control, optimization and data analytics of future power networks with more renewable energy. *J Cleaner Prod* 2021;301:126877. <http://dx.doi.org/10.1016/j.jclepro.2021.126877>.
- Beyza J, Yusta JM. The effects of the high penetration of renewable energies on the reliability and vulnerability of interconnected electric power systems. *Reliab Eng Syst Saf* 2021;215:107881. <http://dx.doi.org/10.1016/j.res.2021.107881>.
- Adedipe T, Shafiee M, Zio E. Bayesian network modelling for the wind energy industry: An overview. *Rel Eng Syst Saf* 2020;202:107053. <http://dx.doi.org/10.1016/j.res.2020.107053>.
- Gandoman FH, Ahmadi A, den Bossche PV, Van Mierlo J, Omar N, Nezhad AE, et al. Status and future perspectives of reliability assessment for electric vehicles. *Rel Eng Syst Saf* 2019;183:1–16. <http://dx.doi.org/10.1016/j.res.2018.11.013>.
- Zarei T, Morozovska K, Laneryd T, Hilber P, Wihlén M, Hansson O. Reliability considerations and economic benefits of dynamic transformer rating for wind energy integration. *Int J Electr Power Energy Syst* 2019;106:598–606. <http://dx.doi.org/10.1016/j.ijepes.2018.09.038>.
- Liserre M, Buticchi G, Leon JI, Alcaide AM, Raveendran V, Ko Y, et al. Power routing: a new paradigm for maintenance scheduling. *IEEE Ind Electron Mag* 2020;14(3):33–45.
- Gilbert C, Browell J, McMillan D. Leveraging turbine-level data for improved probabilistic wind power forecasting. *IEEE Trans Sustain Energy* 2019;1. <http://dx.doi.org/10.1109/TSTE.2019.2920085>.
- Wang F, Du J, Zhao Y, Tang T, Shi J. A deep learning based data fusion method for degradation modeling and prognostics. *IEEE Trans Reliab* 2021;70(2):775–89. <http://dx.doi.org/10.1109/TR.2020.3011500>.
- Fink O, Wang Q, Svensén M, Dersin P, Lee W-J, Ducoffe M. Potential, challenges and future directions for deep learning in prognostics and health management applications. *Eng Appl Artif Intell* 2020;92:103678. <http://dx.doi.org/10.1016/j.engappai.2020.103678>.
- Viana FA, Subramaniyan AK. A survey of Bayesian calibration and physics-informed neural networks in scientific modeling. *Arch Comput Methods Eng* 2021;28:3801–3830. <http://dx.doi.org/10.1007/s11831-021-09539-0>.
- Arias Chao M, Kulkarni C, Goebel K, Fink O. Fusing physics-based and deep learning models for prognostics. *Reliab Eng Syst Saf* 2022;217:107961. <http://dx.doi.org/10.1016/j.res.2021.107961>.
- Nascimento RG, Corbetta M, Kulkarni CS, Viana FA. Hybrid physics-informed neural networks for lithium-ion battery modeling and prognosis. *J Power Sources* 2021;513:230526. <http://dx.doi.org/10.1016/j.jpowsour.2021.230526>.
- Zang Y, Shanguan W, Cai B, Wang H, Pecht MG. Hybrid remaining useful life prediction method. a case study on railway D-cables. *Reliab Eng Syst Saf* 2021;213:107746. <http://dx.doi.org/10.1016/j.res.2021.107746>.
- Chiachío J, Jalón ML, Chiachío M, Kolios A. A Markov chains prognostics framework for complex degradation processes. *Reliab Eng Syst Saf* 2020;195:106621. <http://dx.doi.org/10.1016/j.res.2019.106621>.
- Si X-S, Li T, Zhang J, Lei Y. Nonlinear degradation modeling and prognostics: A box-cox transformation perspective. *Reliab Eng Syst Saf* 2022;217:108120. <http://dx.doi.org/10.1016/j.res.2021.108120>.
- Chen J, Yuan S, Sbarufatti C, Jin X. Dual crack growth prognosis by using a mixture proposal particle filter and on-line crack monitoring. *Reliab Eng Syst Saf* 2021;215:107758. <http://dx.doi.org/10.1016/j.res.2021.107758>.
- Gneiting T, Katzfuss M. Probabilistic forecasting. *Annu Rev Stat Appl* 2014;1:125–51.
- Agoua XG, Girard R, Kariniotakis G. Probabilistic models for spatio-temporal photovoltaic power forecasting. *IEEE Trans Sustain Energy* 2019;10(2):780–9. <http://dx.doi.org/10.1109/TSTE.2018.2847558>.
- Volkanovski A. Wind generation impact on electricity generation adequacy and nuclear safety. *Reliab Eng Syst Saf* 2017;158:85–92. <http://dx.doi.org/10.1016/j.res.2016.10.003>.

- [35] Yeratapally SR, Glavicic MG, Argyrakis C, Sangid MD. Bayesian uncertainty quantification and propagation for validation of a microstructure sensitive model for prediction of fatigue crack initiation. *Reliab Eng Syst Saf* 2017;164:110–23. <http://dx.doi.org/10.1016/j.res.2017.03.006>.
- [36] Aizpurua JI, Catterson VM, Stewart BG, McArthur SDJ, Lambert B, Cross JG. Uncertainty-aware fusion of probabilistic classifiers for improved transformer diagnostics. *IEEE Trans Syst Man Cybern: Syst* 2021;51(1):621–33. <http://dx.doi.org/10.1109/TSMC.2018.2880930>.
- [37] Hughes W, Zhang W, Bagtzoglou AC, Wanik D, Pensado O, Yuan H, et al. Damage modeling framework for resilience hardening strategy for overhead power distribution systems. *Reliab Eng Syst Saf* 2021;207:107367. <http://dx.doi.org/10.1016/j.res.2020.107367>.
- [38] Rocchetta R, Patelli E. A post-contingency power flow emulator for generalized probabilistic risks assessment of power grids. *Reliab Eng Syst Saf* 2020;197:106817. <http://dx.doi.org/10.1016/j.res.2020.106817>.
- [39] Winkler RL, Grushka-Cockayne Y, Jr. KCL, Jose VRR. Probability forecasts and their combination: A research perspective. *Decis Anal* 2019;16(4):239–60. <http://dx.doi.org/10.1287/deca.2019.0391>.
- [40] Aizpurua JI, McArthur S, Stewart B, Lambert B, Cross JG, Catterson VM. Adaptive power transformer lifetime predictions through machine learning and uncertainty modeling in nuclear power plants. *IEEE Trans Ind Electron* 2019;66(6):4726–37. <http://dx.doi.org/10.1109/TIE.2018.2860532>.
- [41] Aizpurua JI, Garro U, Muxika E, Mendicute M, Gilbert IP, Stewart BG, et al. Probabilistic power transformer condition monitoring in smart grids. In: 2019 6th int. advanced research workshop on transformers. 2019, p. 42–7. <http://dx.doi.org/10.23919/ARWtr.2019.8930193>.
- [42] Gneiting T, Katzfuss M. Probabilistic forecasting. *Annu Rev Stat Appl* 2014;1(1):125–51. <http://dx.doi.org/10.1146/annurev-statistics-062713-085831>.
- [43] Hong T, Pinson P, Fan S, Zareipour H, Troccoli A, Hyndman RJ. Probabilistic energy forecasting: Global energy forecasting competition 2014 and beyond. *Int J Forecast* 2016;32(3):896–913. <http://dx.doi.org/10.1016/j.ijforecast.2016.02.001>.
- [44] Verbois H, Rusydi A, Thiery A. Probabilistic forecasting of day-ahead solar irradiance using quantile gradient boosting. *Sol Energy* 2018;173:313–27. <http://dx.doi.org/10.1016/j.solener.2018.07.071>.
- [45] Meinshausen N. Quantile regression forests. *J Mach Learn Res* 2006;7:983–99.
- [46] Friedman JH. Greedy function approximation: a gradient boosting machine. *Ann Statist* 2001;1189–232.
- [47] Arulampalam MS, Maskell S, Gordon N, Clapp T. A tutorial on particle filters for online nonlinear/non-Gaussian Bayesian tracking. *IEEE Trans Signal Process* 2002;50(2):174–88. <http://dx.doi.org/10.1109/78.978374>.
- [48] Heathcote MJ. J & P transformer book. Thirteenth ed.. Newnes; 2007. <http://dx.doi.org/10.1016/B978-075068164-3/50008-9>.
- [49] IEEE PES. IEEE guide for loading mineral-oil-immersed transformers and step-voltage regulators. IEEE; 2011, Std. C57.91.
- [50] Bicen Y, Aras F, Kirkici H. Lifetime estimation and monitoring of power transformer considering annual load factors. *IEEE Trans Dielectr Electr Insul* 2014;21(3):1360–7.
- [51] Ariannik M, Razi-Kazemi AA, Lehtonen M. An approach on lifetime estimation of distribution transformers based on degree of polymerization. *Rel Eng Sys Safety* 2020;198:106881. <http://dx.doi.org/10.1016/j.res.2020.106881>.
- [52] Catterson V. Prognostic modeling of transformer aging using Bayesian particle filtering. In: Electrical insulation and dielectric phenomena (CEIDP), 2014 IEEE conference on. 2014, p. 413–6. <http://dx.doi.org/10.1109/CEIDP.2014.6995874>.
- [53] Li S, Ma H, Saha TK, Yang Y, Wu G. On particle filtering for power transformer remaining useful life estimation. *IEEE Trans Power Deliv* 2018;33(6):2643–53. <http://dx.doi.org/10.1109/TPWRD.2018.2807386>.
- [54] Sankaraman S, Goebel K. Uncertainty in prognostics and systems health management. *Int J Prognost Health Manag* 2015;6(10):14.
- [55] Zhu S-P, Huang H-Z, Peng W, Wang H-K, Mahadevan S. Probabilistic physics of failure-based framework for fatigue life prediction of aircraft gas turbine discs under uncertainty. *Reliab Eng Syst Saf* 2016;146:1–12.
- [56] van Schijndel A, Wouters PAAF, Wetzler JM. Modeling of replacement alternatives for power transformer populations. *IEEE Trans Power Deliv* 2012;27(2):506–13. <http://dx.doi.org/10.1109/TPWRD.2011.2181541>.
- [57] IEEE Power and Energy Society. IEEE guide for the interpretation of gases generated in mineral oil-immersed transformers. IEEE; 2019, Std. C57.104.
- [58] Sankaraman S. Significance, interpretation, and quantification of uncertainty in prognostics and remaining useful life prediction. *Mech Syst Signal Process* 2015;52–53:228–47. <http://dx.doi.org/10.1016/j.ymssp.2014.05.029>.
- [59] Kabir S, Papadopoulos Y. A review of applications of fuzzy sets to safety and reliability engineering. *Internat J Approx Reason* 2018;100:29–55.
- [60] Duan K-B, Rajapakse JC, Wang H, Azuaje F. Multiple SVM-RFE for gene selection in cancer classification with expression data. *IEEE trans nanobiosci* 2005;4(3):228–34.
- [61] Yan K, Zhang D. Feature selection and analysis on correlated gas sensor data with recursive feature elimination. *Sensors Actuators B* 2015;212:353–63.
- [62] Hersbach H. Decomposition of the continuous ranked probability score for ensemble prediction systems. *Weather Forecast* 2000;15(5):559–70. [http://dx.doi.org/10.1175/1520-0434\(2000\)015<0559:DOTCRP>2.0.CO;2](http://dx.doi.org/10.1175/1520-0434(2000)015<0559:DOTCRP>2.0.CO;2).
- [63] Gneiting T, Raftery AE, Westveld III AH, Goldman T. Calibrated probabilistic forecasting using ensemble model output statistics and minimum CRPS estimation. *Mon Weather Rev* 2005;133(5):1098–118.
- [64] Karlsson R, Schon T, Gustafsson F. Complexity analysis of the marginalized particle filter. *IEEE Trans Signal Process* 2005;53(11):4408–11.
- [65] Xu Q-S, Liang Y-Z. Monte Carlo cross validation. *Chemometr Intell Lab Syst* 2001;56(1):1–11.
- [66] Kuhn M, Johnson K, et al. Applied predictive modeling. Vol. 26. New York: Springer; 2013.
- [67] Marcot BG, Hanea AM. What is an optimal value of k in k-fold cross-validation in discrete Bayesian network analysis? *Comput Statist* 2020;1–23.
- [68] Gal Y, Ghahramani Z. Dropout as a Bayesian approximation: Representing model uncertainty in deep learning. In: Balcan MF, Weinberger KQ, editors. Proceedings of the 33rd international conference on machine learning. Proceedings of machine learning research, vol.48, PMLR; 2016, p. 1050–9.
- [69] Abdar M, Pourpanah F, Hussain S, Rezaadegan D, Liu L, Ghavamzadeh M, et al. A review of uncertainty quantification in deep learning: Techniques, applications and challenges. *Inf Fusion* 2021;76:243–97. <http://dx.doi.org/10.1016/j.inffus.2021.05.008>.
- [70] Peng W, Ye Z-S, Chen N. Bayesian deep-learning-based health prognostics toward prognostics uncertainty. *IEEE Trans Ind Electron* 2020;67(3):2283–93. <http://dx.doi.org/10.1109/TIE.2019.2907440>.
- [71] Zhou T, Han T, Droguett EL. Towards trustworthy machine fault diagnosis: A probabilistic Bayesian deep learning framework. *Reliab Eng Syst Saf* 2022;224:108525. <http://dx.doi.org/10.1016/j.res.2022.108525>.